THE ASTROPHYSICAL JOURNAL, 407:723–732, 1993 April 20

THE ASYMMETRIC WIND OF R127

R. E. SCHULTE-LADBECK,[1,2] C. LEITHERER,[3,4,5] G. C. CLAYTON,[2,6] C. ROBERT,[3] M. R. MEADE,[7]
L. DRISSEN,[3] A. NOTA,[3,5] AND W. SCHMUTZ[8]

Received 1992 July 28; accepted 1992 October 15

ABSTRACT

We present optical, linear polarimetry in broad-band *UBVRI* filters plus narrow-band filters centered on the emission lines of Hα and the red [N II] and spectropolarimetry in the wavelength range from 4120 Å to 6770 Å of the luminous blue variable R127 in the Large Magellanic Cloud. Both observations display a decrease of the percentage polarization across the Hα emission line with respect to the continuum. We assume that Hα is recombination-line dominated and thus intrinsically unpolarized, and we use the continuum-subtracted line polarization to estimate the interstellar foreground polarization. The resulting amount of intrinsic continuum polarization of R127 is very large, of order 1%–1.5%, implying both the presence of copious free electrons and a considerable asphericity in their distribution. The two data sets, taken 2 months apart, display significant variations in the continuum polarization, which confirms that the stellar-wind properties of R127 are time-dependent in the maximum state. We discuss several possible wind geometries and present arguments favoring a clumpy, axisymmetric outflow.

Subject headings: Magellanic Clouds — polarization — stars: mass loss — stars: individual (R127) — stars: supergiants

1. INTRODUCTION

Luminous blue variables (LBVs; Conti 1984) are blue supergiants which are located in the Hertzsprung-Russell diagram very near the empirical upper luminosity boundary of stars recognized as the Humphreys-Davidson limit (Humphreys & Davidson 1979). A famous example is η Car, the most luminous star known in the Galaxy (Humphreys & Davidson, Fig. 3). The galactic LBVs are surrounded by resolved, asymmetric nebulosities. Examples are the "homunculus" nebula around η Car (Gaviola 1950), the elliptical ring nebula and the bipolar, helical structures resolved near AG Car (Thackeray 1950; Paresce & Nota 1989), the arc-shaped, bipolar nebula of HR Car (Hutseméker & Van Drom 1991a), the structured nebulosities associated with P Cyg (Johnson et al. 1992) and WRA 751 (Hutseméker & Van Drom 1991b), and the elliptical ring nebula surrounding the possible LBV He 3-519 (Stahl 1987). It is believed that these nebulae were ejected during large outbursts of unknown recurrence rate which LBVs suffer as they encounter an as yet unidentified stability limit of their photospheres (see Lamers & de Loore 1987).

R127 was classed as a peculiar Of supergiant or WN9 star (Walborn 1977, 1982) until it was discovered in 1982 by Stahl et al. (1983) to display the photometric and spectroscopic properties typical of an LBV entering the phase of visual maximum light. The star is currently still at maximum (see below). A full variability cycle has not yet been observed for R127, so we do not know the boundary spectral types/temperatures. The premaximum-state spectra of Stahl et al. showed multiple high- and low-velocity components in the P Cygni profiles of He I lines which displayed complex changes during an intermittent decline in brightness; the high-velocity wings were not present in Walborn's data taken at minimum light. In order to explain these profiles, Lamers (1987) suggested that there developed a deviation of the outflow from spherical symmetry.

Stahl et al. detected nebular lines in the spectrum of a neighboring star to R127 separated by 3″ on the sky and suggested that this could be extended emission from a nebula around R127. Spectroscopy through a 2″ × 6″ aperture with high spectral and spatial resolution obtained by Appenzeller, Wolf, & Stahl (1987) during the subsequent brightness increase of R127 in 1986 indeed revealed a resolved, gaseous nebula with an angular diameter of 4″ in east–west direction, corresponding to a linear extension of about 1 pc at the distance of the LMC. From the spatial distribution of the emission, Appenzeller et al. inferred that "there are obviously deviations from spherical symmetry or/and obscuration effects." Stahl (1987) obtained narrow-band CCD images of R127 centered on nebular emission lines. Resolving the shell with imaging was a difficult observation, because it is both small and close to a bright star. Stahl found the image of R127 to be slightly more extended than the stellar point-spread function in [N II] λ6584. We note that the point-spread-function–corrected image is suggestive of a bipolar enhancement of the emission at a position angle of ~110°. Attempts to image the matter within a few arcseconds around R127 in the visual continuum with the STScI coronograph (Nota et al. 1991) resulted in the detection of several neighboring stars, but no nebular features. Consequently there appears to be no scattered continuum light, and no such structures like the helical "jet" discovered with the same instrument around the LBV AG Car (Paresce & Nota 1989). Recent, new coronographic images of R127 taken in a 110 Å wide filter

[1] Department of Physics and Astronomy, University of Pittsburgh, 3941 O'Hara Street, Pittsburgh, PA 15260.
[2] Visiting Astronomer at the Anglo-Australian Telescope which is operated by the Anglo-Australian Observatory.
[3] Space Telescope Science Institute, 3700 San Martin Drive, Baltimore, MD 21218.
[4] Visiting Astronomer at the European Southern Observatory, La Silla, Chile.
[5] Affiliated with the Astrophysics Division of the Space Science Department of ESA.
[6] Center for Astrophysics and Space Astronomy, University of Colorado, Campus Box 389, Boulder, CO 80309.
[7] Space Astronomy Laboratory, University of Wisconsin, 1150 University Avenue, Madison, WI 53706.
[8] Institut für Astronomie, ETH-Zentrum, CH-8092 Zürich, Switzerland.

centered on Hα confirm the bipolar emission hinted at in Stahl's [N II] image (Clampin et al. 1992). The nebula is detected to angular distances of 8″ × 9″ from the star corresponding to linear sizes of 1.9 pc × 2.2 pc. The opening angle for both emission patches is found to be almost 90° and the position angle is 95°–100°. The shell is inferred to be $\sim 4 \times 10^4$ yr old (Clampin et al.) so it was ejected before the current episode of activity.

Could there possibly be a causal connection between the deviations from spherical symmetry seen in the old shell and those suggested to be present in the stellar wind nowadays? A very sensitive means to probe the distribution of material very close to a star is by measuring its linear polarization. Hayes (1985), Lupie & Nordsieck (1987), and Taylor et al. (1991) used time-dependent polarimetry across the optical spectrum of the LBV P Cyg to demonstrate that its electron density distribution is asymmetric and also varies measureably on time scales as short as 1 day. In this paper, we present and discuss the first wavelength-dependent polarimetry of R127 and discuss implications for the stellar-wind geometry.

2. OBSERVATIONS

Our first set of polarimetric observations of R127 was obtained on 1991 September 18 with the PISCO polarimeter attached to the ESO 2.2 m telescope. We used *UBVRI* filters, as well as two narrow-band filters centered at 6562 Å with a width (FWHM) of 12.4 Å for measuring Hα, and at 6585 Å with a width of 23.8 Å for measuring the red [N II] line. The observations were taken through a pair of 7″ circular apertures separated by 80″ on the sky. They were calibrated against a set of standard-star observations obtained during the 3 day observing run. We obtained the instrumental efficiency by inserting a polaroid into the beam. The instrumental polarization was determined from multiple observations of the unpolarized standard star ϵ Ind and was significant only in the *U* filter. The zero point of the position angle was derived from observations of the highly polarized standard star σ Sco, for which we assumed a constant position angle of 32°.9 as a function of wavelength. The reduced data are listed in Table 1 and plotted in Figure 1.

The possible large change of polarization at Hα suggested at the 1 σ level in the PISCO data motivated a second observation. It was taken on 1991 November 27 with the half-wave, CCD polarimeter of the 3.9 m AAT. A "double-dekker" with an aperture size of 2″.7 and a separation on the sky of 25″ was used to record simultaneously the star and sky spectra; the seeing was 3″. The images were bias-subtracted using the overscan area of the CCD, a two-dimensional wavelength calibration was copied onto the data, then the spectra were subtracted and two sets of alternating star-sky spectra at four

TABLE 1

FILTER-POLARIZATION DATA

λ_c (Å)	HWHM (Å)	PA (°)	*P* (%)	σ (%)	*Q* (%)	*U* (%)
3523.....	186	53.0	0.53	0.11	−0.15	0.51
4425.....	500	49.6	0.83	0.08	−0.13	0.82
5320.....	520	47.2	0.94	0.05	−0.07	0.94
5916.....	737	46.6	0.88	0.05	−0.05	0.87
8044.....	1720	48.4	0.72	0.08	−0.09	0.72
6562.....	6.2	10.8	0.19	0.52	0.18	0.07
6585.....	11.9	48.6	0.79	0.32	−0.10	0.78

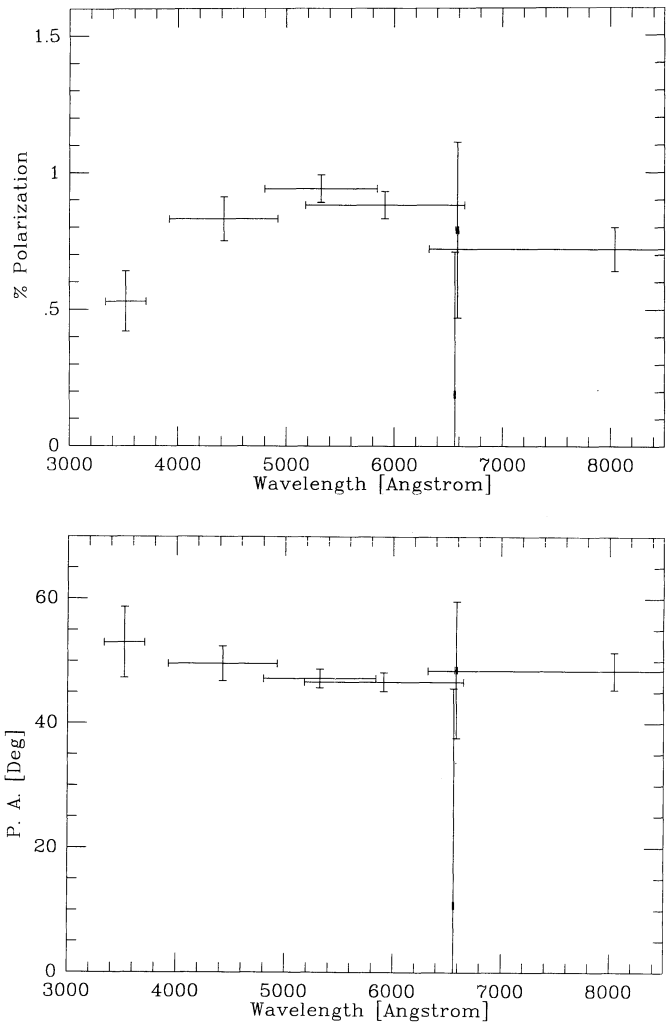

FIG. 1.—The percentage polarization and position angle of the filter observations taken on 1991 September 18 with PISCO are plotted as a function of wavelength. The vertical error bars are the ±1 σ errors of the measurements; the horizontal bars indicate the FWHM of the filter that was used.

wave-plate positions were combined to give the spectra of the three observed Stokes parameters. The observations cover a wavelength region from 4120 Å to 6770 Å. The expected resolution as calculated from the projected slit width is ∼9 Å (FWHM); the sampling of the data was 2.7 Å pixel^{-1}. The instrumental polarization was determined from an observation of the nearby bright star BS 1294, and at 0.02% was found to be negligible. The instrumental efficiency and zero point of the position angle were measured by inserting an HN22 polaroid into the beam, which has an efficiency greater than 99.9% over the spectral range used for the observations. The data show a low-frequency variation of the position angle owing to wavelength-dependent position-angle variations intrinsic to the wave plate. The polarization reduction software allows for fitting of a polynomial of adjustable order to the position-angle measurement, and this fit was used to eliminate the position-angle dependence of the wave plate in the data. It was not possible to achieve a perfectly flat position-angle calibration across the whole spectrum within the possible fit parameters; there remained a systematic error with an amplitude of about ±1°.5. A control measurement was performed on the highly

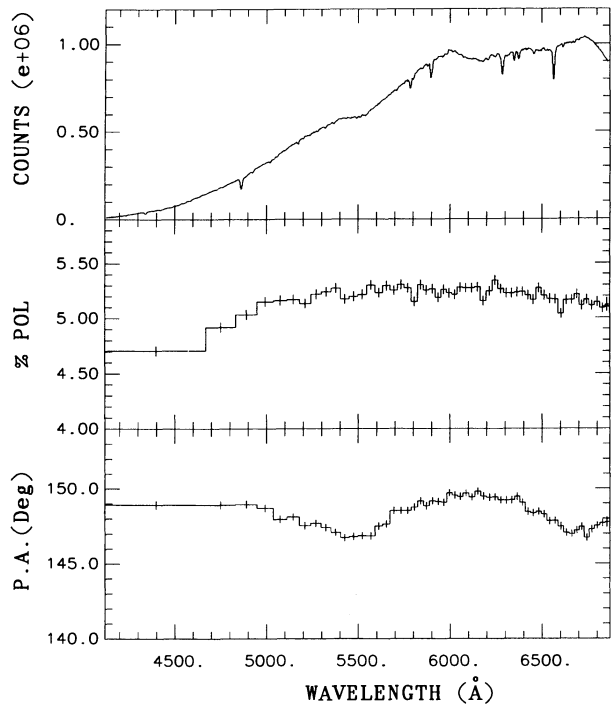

FIG. 2.—The counts, percentage polarization, and position angle of the highly polarized standard star HD 298383 as observed with the AAT spectropolarimeter are displayed as a function of wavelength, in order to show the quality of the calibration and to illustrate the systematic errors in the position angle (data should be flat). The polarization data were binned to a constant error of 0.05%; therefore, a variable spectral resolution results.

polarized standard star HD 298383 and yielded the expected result. Our data for HD 298383 are shown in Figure 2 in order to illustrate the quality of the calibration and the nature of the systematic errors. The reduced observations of R127 are displayed in Figure 3. The polarization data were binned to a constant error of 0.05% polarization, and thus exhibit a spectral resolution which is dependent on the registered counts.

3. RESULTS

A list of the observed positions and possible identifications of emission and absorption lines in the rich spectrum of R127, together with a qualitative indication of their strengths, is given as Table 2. The spectrum of R127 was governed by the very strong emission line of Hα, with an equivalent width of 42 Å. Hα was blended in the red wing with [N II] λ6584, which had a strength of about a fifth that of Hα. In the blue wing, it was blended with an emission line of Fe II (40) λ6516 (the blue [N II] line was not resolved). The ratio of Hα to Hβ was quite large, and we did not detect Hγ. This is likely due to filling in of the underlying "pseudophotospheric" Balmer absorption with emission from the wind and surrounding H II region. Longward of Hα, the pair of [S II] lines was observed at a line ratio between 0.5 and 1, indicating an electron density of about 10^3 cm^{-3}. At the low resolution of our spectrum, it is difficult in some regions to define the continuum, i.e., to distinguish whether or not there is an absorption feature or an emission feature present, and to discern P Cygni absorption troughs from weak emissions. The spectrum was clearly very rich in metal lines. There is a problem of blending in the crowded Fe II line regions between about 5100 to 5300 Å. Some emission lines could be identified with [Fe II] lines just as well as with Fe II lines, however, at our resolution, the identifications of individual lines are not certain. Other metal lines found in the spectrum can be ascribed to neutral oxygen, singly ionized titanium, chromium, and silicon, and to neutral and singly ionized magnesium and nitrogen. The Na I D lines formed the strongest absorption feature in our spectrum (EW ~ 2 Å). High-resolution spectroscopy has revealed three major components of Na I D absorption toward R127 (Stahl & Wolf 1986), interstellar Galactic and LMC and circumstellar, respectively. At the resolution of our spectra, all of the components previously seen in these lines are blended together. Several other, weak interstellar lines are cataloged in Table 2. There is an absorption feature which seemingly coincides with He I λ6678. However, we did not detect He I λ5876, which should be located in the blue wing of Na I D, or other He I lines. On the other hand, it is possible that He I λ5876 was filled in by emission and thus went undetected. He II λ4686 was truant as well.

Figures 1 and 3 disclose that there is a change of the percentage polarization (%P) and the position angle (PA) across the Hα emission line, which is statistically significant in the AAT data. This immediately indicates the presence of intrinsic continuum polarization in R127 (see below). The broad-band data are fairly constant with wavelength, except for the U filter datum, which is lower in %P but does not exhibit a significantly different PA when compared with, e.g., the B filter observation. The polarization measurement for the [N II] line is in agreement with the measurements in the R and I filters, probably because the line was too weak to dilute the continuum polarization. The strength of the [N II] line is about one-fifth that of Hα, while the filter was twice as wide; thus we

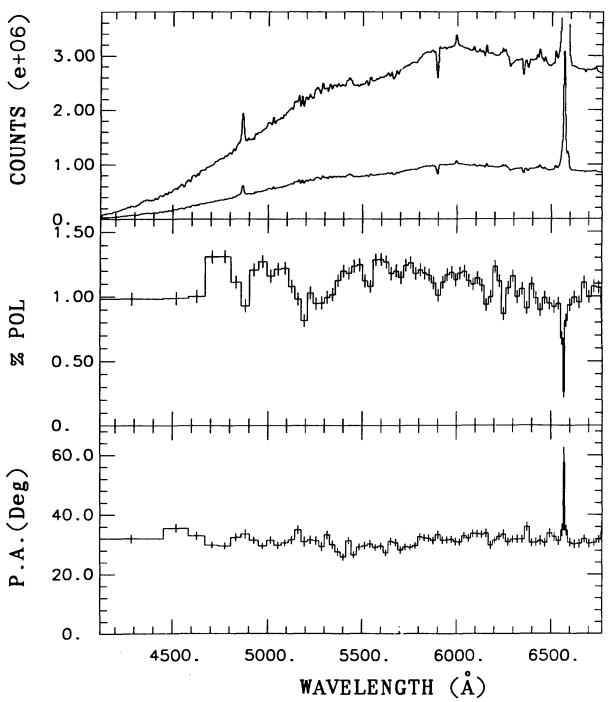

FIG. 3.—The counts, percentage polarization, and position angle of R127 observed on 1991 November 27 with the AAT spectropolarimeter as a function of wavelength. The counts spectrum is overplotted at a magnified scale to bring out the copious weak emission lines which are mostly due to Fe. The polarization data were binned to a constant error of 0.05%; thus a variable resolution results. Note the significant change of polarization at the strong Hα emission line.

TABLE 2

SPECTROSCOPY

λ_{obs} (Å)	Quality[a]	Identifications
4274.....	a, w	
4283.....	e, w	
4299.....	a, w	Ti II (20) 4294.1, Ti II (41) 4300.1
4363.....	e, w	
4409.....	e, w	
4417.....	a, w, P	Fe II (27) 4416.8
4436.....	e, w	
4445.....	a, w	Ti II (19) 4443.8
4461.....	e, w	
4470.....	a, w	Ti II (31) 4468.5
4477.....	e, w	
4487.....	a, w	Fe II (37) 4491.4, Mg II (4) 4481.2
4512.....	e, w	Fe II (38) 4508.3, Fe II (37) 4515.3
4520.....	a, w	Fe II (37) 4520.2, Fe II (38) 4522.6
4543.....	e, w	
4555.....	a, w, P	Fe II (38) 4549.5, Fe II (37) 4555.9, Cr II (44) 4558.7
4570.....	e, w	Fe II (38) 4549.5, Fe II (37) 4555.9, Cr II (44) 4558.7
4589.....	a, w, P	Fe II (38) 4583.8, Cr II (44) 4588.2
4610.....	e, w	
4619.....	a, w	
4634.....	a, w	Fe II (37) 4629.3
4774.....	e, w	[Fe II] (4F) 4772.1
4799.....	e, w	[Fe II] (4F) 4798.3, 4799.3
4806.....	a, w	
4818.....	e, w	
4825.....	a, w	Cr II (30) 4824.1
4843.....	e, w	[Fe II] (3F) 4843.5
4865.....	e, s	H I (1) 4861.3
4894.....	e, w	[Fe II] (4F) 4889.6, [Fe II] (3F) 4889.7
4917.....	e, w	[Fe II] (3F) 4917.2
4934.....	e, w	N I (9) 4935.0
5000.....	e, m	blend
5025.....	e, m	[Fe II] (20 F) 5020.2
5034.....	a, w	
5050.....	e, w	
5066.....	e, w	
5072.....	a, w	
5081.....	e, w	
5089.....	a, w	
5129.....	a, w	
5138.....	e, w	blend
5419.....	e, w	blend
5163.....	e, m	[Fe II] (19F) 5158.8
5170.....	a, m	Mg I (2) 5167.3, 5172.7, 5183.6
5179.....	e, m	[Fe II] (18F) 5182.0
5189.....	a, m	
5200.....	e, w	Fe II (49) 5197.6
5209.....	a, w	
5220.....	e, m	
5235.....	a, w	Fe II (49) 5234.6
5257.....	e, m	blend, Fe II (41) 5256.9, [Fe II] (19F) 5261.6
5276.....	a, m	Fe II (49) 5276.0
5288.....	e, m	Fe II (41) 5284.1
5315.....	a, m, P	Fe II (49) 5316.6, Fe II (48) 5316.8
5325.....	e, m	Fe II (49) 5316.6, Fe II (48) 5316.8
5338.....	a, w	
5347.....	e, w	blend
5361.....	a, w, P	Fe II (48) 5362.9
5371.....	e, w	Fe II (48) 5362.9
5384.....	a, w	
5390.....	e, w	
5419.....	e, m	blend, [Fe II] (16F) 5413.3
5429.....	e, m	blend, Fe II (49) 5425.3
5479.....	a, w	
5519.....	e, w	
5527.....	a, m	
5540.....	e, m	
5571.....	e, w	
5593.....	e, w	
5632.....	e, m	
5640.....	a, m	
5651.....	e, m	[Fe II] (39F) 5649.7, 5650.9
5663.....	a, m	
5677.....	e, m	N II (3) 5666.6, 5676.0, 5679.6
5688.....	a, m	
5782.....	a, w	Interstellar features 5778.3, 5780.4
5856.....	a, w	
5867.....	e, w	
5877.....	a, w	
5895.....	a, s	Na I (1) 5890.0, 5895.9
5908.....	e, w	
5942.....	a, w	
5995.....	e, s	Fe II (46) 5991.4
6088.....	e, m	Fe II (46) 6084.1
6117.....	e, w	Fe II (46) 6113.3
6134.....	e, w	
6145.....	a, m	
6153.....	e, m	O I (10) 6156.0, 6156.8, 6158.2
6183.....	e, w	
6231.....	e, w	blend
6241.....	e, m	blend
6245.....	e, m	blend, Fe II (74) 6247.6
6279.....	a, m	Interstellar features 6269.8, 6283.9
6348.....	a, m	Si II (2) 6347.1
6373.....	a, m	Fe II (40) 6369.5, Si II (2) 6371.4
6423.....	e, w	N I (23) 6420.5
6436.....	e, m	Fe II (40) 6432.7, N I (23) 6441.7
6464.....	e, m	Fe II (74) 6456.4, N I (22) 6457.9, 6468.3
6521.....	e, m	Fe II (40) 6516.1
6568.....	e, s	H I (1) 6562.8
6586.....	e, s	[N II] (1) 6583.6
6678.....	a, w	
6723.....	e, w	[S II] (2) 6717.0
6736.....	e, w	[S II] (2) 6731.3

[a] e = emission, a = absorption, P = possible P Cygni trough, w = weak, m = moderate, s = strong.

would expect the polarization change to be 1/10 of that observed at Hα. This is consistent with the data. In addition, Figure 3 shows depressions of the $\%P$ at the Fe II line region and at Hβ, but with no apparent PA rotation. A slight rotation of the PA at Hβ can be seen when a different binning is used, in the same direction as that which is observed in Hα. A measurement of the polarization in a 13 Å wide bandpass centered on Hβ reveals that the polarization in the line itself with the continuum subtracted is different from the polarization of the underlying continuum. The difference is statistically significant, 4.2 σ in Q and 5.5 σ in U. There seems to be a dip in $\%P$ at the Na I D lines. As noted above, the Na I D lines in R127 have both interstellar (Galactic and LMC) and circumstellar components of different strengths (Stahl & Wolf 1986), all of which are blended together in our spectrum. While the interstellar components are not expected to cause a polarization change as the photons are scattered from an isotropic radiation field, rescattering of polarized light in the circumstellar lines might be contrived to result in a polarization variation. Finally, the polarization shortward of Hα down to about 6100 Å appears to be more noisy than one would expect from the errors. Some of these features in the polarization are likely to be real,

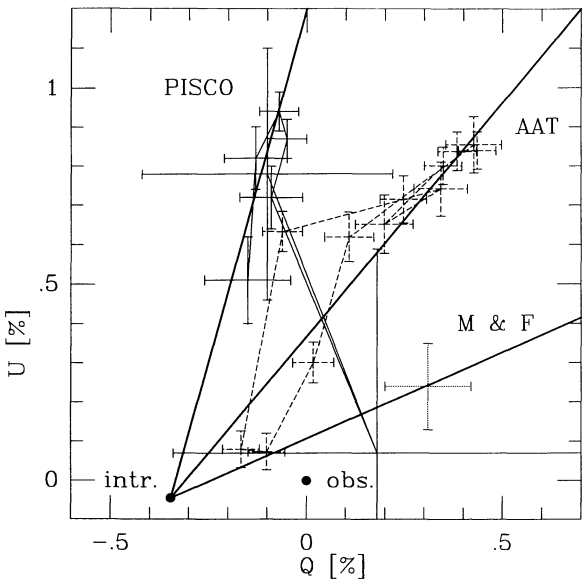

FIG. 4.—*Q-U* diagram showing the filter polarimetry (PISCO), the spectropolarimetry across Hα with its blue and redward continuum (AAT), and the white-light data point of Mathewson & Ford (M&F). Data points in the multispectral sets were connected with increasing wavelength. The zero point of the diagram in the observed frame is labeled "obs.," while the inferred zero point at 5600 Å in the intrinsic frame is labeled "intr." Heavy lines were drawn from the intrinsic zero point through the mean locations of the three data sets, to illustrate the intrinsic variations of amount of polarization and position angle of R127.

because the spectrum displays many weak lines which are recorded at a high count level. However, the signal-to-noise ratio is too small to unambigously identify specific features.

In Figure 4, we plotted in a *Q-U* diagram the filter-polarimetry data, the polarization across Hα and the adjacent continuum from the spectropolarimetry (plotting all of the spectrum would lead to overcrowding of the diagram), and the data point of Mathewson & Ford (1970) who reported a polarization of 0.39% (±0.11%) at 19 (±8°) in white light (no filter, photocathode detector) obtained in a 1969/1970 survey of the Magellanic Clouds. The spectropolarimetric data are unbinned across the line (e.g., pixel-by-pixel values are graphed). The polarization decrease to line center and recovery to the continuum level is very rapid; the line was not resolved in flux, nor in polarization. The *U* filter polarization decreases as mentioned above, along the same PA as the Hα polarization. The polarization in the continuum is noticed to be variable as a function of time.

The observed polarization of R127 is expected to contain at least two components, the intrinsic polarization and the interstellar foreground polarization (ISP) on the sight line to R127. The broad-band observations covering a large fraction of the spectrum reveal that excluding the *U* and the narrow-band data, the %*P* and PA wavelength dependence is consistent with being a constant, or that there is only a very slight curvature to the %*P* as well as a gradual rotation of the PA as a function of wavelength. The %*P* wavelength dependence of the broad-band data is not consistent with a Serkowski law. If we interpret the data as the superposition of two polarization vectors, it follows both from the overall wavelength dependence and the large decrease of polarization at Hα that the intrinsic polarization dominates the observed polarization.

A technique that is frequently used to determine the ISP is the field-star method. Its assumption is that stars located near the program star in space but which do not have an intrinsic polarization component should provide a measure of the ISP on the sight line in question. We examined the measurements of Mathewson & Ford (1970) and Clayton, Martin, & Thompson (1983) of LMC stars in the vicinity of R127, displayed in Figure 5. Based on all the stars included in a circle of a 1° radius centered on R127, we estimated an average foreground ISP (Galactic plus LMC) at the position of R127 of 0.18% (±0.05%) at 25° (±7°). The polarization vectors of the stars surrounding R127 describe a chaotic pattern which suggests some caution in using the field-star method to derive the average ISP on this sight line. Many of the stars observed by Mathewson & Ford and Clayton et al. are luminous, early-type stars or Wolf-Rayet stars which could show some important, still unknown, intrinsic polarization. This may contribute to the random orientation of the vectors observed in the field around R127.

A different technique to determine the interstellar polarization is one in which the polarization in an emission line is measured. Following McLean (1977) we assume that the stellar wind consists of two layers, one of which is close to the star and highly ionized and which scatters and partially polarizes the stellar continuum flux, while the second and more outlying region predominantly produces the emission-line spectrum via recombination. It is important only to establish that the line emission is unpolarized. It then furnishes us with a source of unpolarized light on the same sight line and at the same distance as the continuum source. (However, if the electron-scattering optical depth in the stellar wind is sufficently high, or if the contribution from the shell to the observed fluxes contains reflected Hα emission, Hα might be polarized.) Including a contribution of photospheric Hα absorption, at some wavelength λ the total intensity, I_T, in such a line is given by

$$I_T(\lambda) = r(\lambda) I_C(\lambda) + I_E(\lambda) , \quad (1)$$

where I_C is the intensity of the continuum, I_E is the intensity of

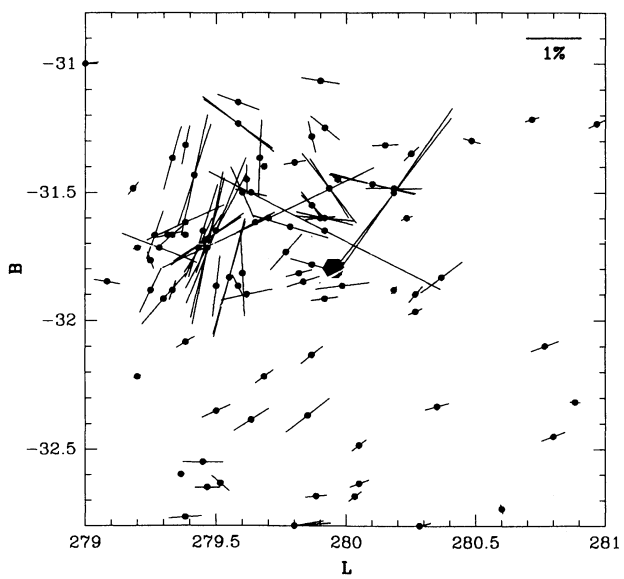

FIG. 5.—A polarization map of field stars in the LMC within 2° of R127. *B* and *L* are the galactic longitude and latitude, respectively. The position of R127 is indicated by the hexagon. The polarization vectors are drawn at the position of the stars.

the line, and r is the residual intensity of the photospheric absorption. (The concept of a photospheric absorption is probably not valid in an object where part of the continuum forms in the stellar wind, because there is no well-defined stellar radius. However, the absence of Hγ emission in our spectrum was suggestive of a competing absorptive component presumably formed in the "pseudophotosphere.") Associating polarization components Q and U with the continuum and line intensities yields

$$\frac{Q_E(\lambda)}{Q_C(\lambda)} = \frac{[Q_T(\lambda)/Q_C(\lambda)][1 + I_E(\lambda)/r(\lambda)I_C(\lambda)] - 1}{I_E(\lambda)/r(\lambda)I_C(\lambda)} \quad (2)$$

and the same for U. We may use this equation to separate the line and continuum polarizations in our spectropolarimetric data set. Assuming that the polarization of Hα is zero, and that the underlying stellar absorption can be neglected, we obtain $Q_E = -0.34\%$ ($\pm 0.06\%$), and $U_E = -0.04\%$ ($\pm 0.06\%$).

The assumption that Hα is unpolarized and merely dilutes the continuum polarization is justifiable for several reasons. First, recombination produces unpolarized emission, while the polarization created by line scattering in Hα is very small (Jeffrey 1991). Second, we do not expect the line to scatter strongly at electrons because it forms over a large volume in the circumstellar environment, whereas the electron density should drop off rapidly as a function of distance from the star. The assumption that we can neglect underlying photospheric absorption in Hα is probably also valid, because the equivalent width of the Hα absorption of very luminous A supergiants is typically less than 5 Å (Kurucz 1979), which is small compared to R127's Hα emission, greater than 42 Å. We empirically verified a contribution less than 10% by absorption to be of no significant consequence to the interstellar polarization correction derived from it.

In the case of the Hβ line, underlying absorption is expected to be a significant contribution. If we model this line with a dilution effect only, we obtain $Q_E = -0.8\%$ ($\pm 0.3\%$), and $U_E = -0.7$ ($\pm 0.3\%$). The polarized flux spectrum (see below) shows an absorption at Hβ having an equivalent width of 1.7 Å. We interpret this as the reflected photospheric absorption. The observed equivalent width is not inconsistent with that which is expected. If we take the underlying absorption into account in our measurement of the line polarization, we derive the polarization parameters $Q_E = -0.4\%$ ($\pm 0.2\%$), and $U_E = -0.2$ ($\pm 0.2\%$) and the Hβ and Hα line polarizations are now in good agreement. The continuum-to-line vectors, which should yield the intrinsic polarization at the time of the AAT observation if both lines are modeled correctly, agree within the errors with each other, as well as with the continuum polarization measured after ISP removal. These results indicate that our model is at least consistent.

The polarization in Hα is thus accepted to yield the value of the ISP component at the wavelength of Hα, although there is a large discrepancy with the value derived from the field-star method. According to Clayton et al., the wavelength dependence of the interstellar polarization in the LMC is not different from Galactic. We used a Serkowski law (Whittet et al. 1992) with the assumption of $\lambda_{max} = 5600$ Å, and $K = 1.84$, to model the ISP on the sight line to R127. The values are $P_{max} = 0.35\%$ at 93°.7.

We subtracted the above ISP. The computed intrinsic polarizations are displayed in Figures 6 and 7. Due to the systematic uncertainties in the ISP correction, we have not propagated

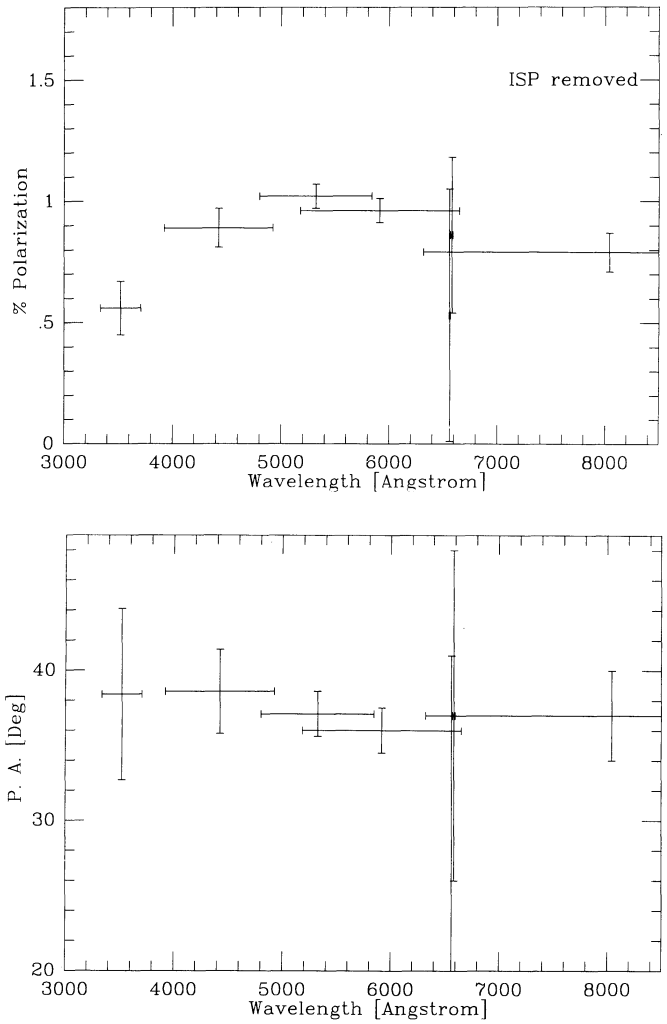

FIG. 6.—Intrinsic polarization of the PISCO data

errors onto our results. The intrinsic polarization is slightly higher than the observed polarization. In the spectropolarimetric data, the $\%P$ at Hα decreases strongly, but the PA change has disappeared. Depressions in $\%P$ at Hβ and the Fe II line region remain, without having created features in the PA spectrum. The overall PA is consistent with a constant at 25°. The filter data show a similar result, but at different $\%P$ and PA levels. The U filter observation remains lower than the other broad-band measurements in $\%P$. We note that this filter bridges the Balmer jump of hydrogen. It is well known that the polarization decreases shortward of the Balmer jump in Be stars. However, it did not change in this fashion in the LBV P Cyg (Taylor et al. 1991) at all times. A similar question arises regarding the I-band datum, which includes the Paschen jump. We cannot discuss the observations in any more detail without knowing the wavelength dependence of the polarization better. However, the late spectral type of R127 suggests that the wind may not have been fully ionized; hence hydrogen absorption competing with electron scattering could have introduced a color-dependent continuum polarization just like in Be stars. We suggest that the polarization in R127 is created by electron scattering and modified by hydrogen line and possibly continuum, and iron line, emission, and absorption processes in the wind and nebula.

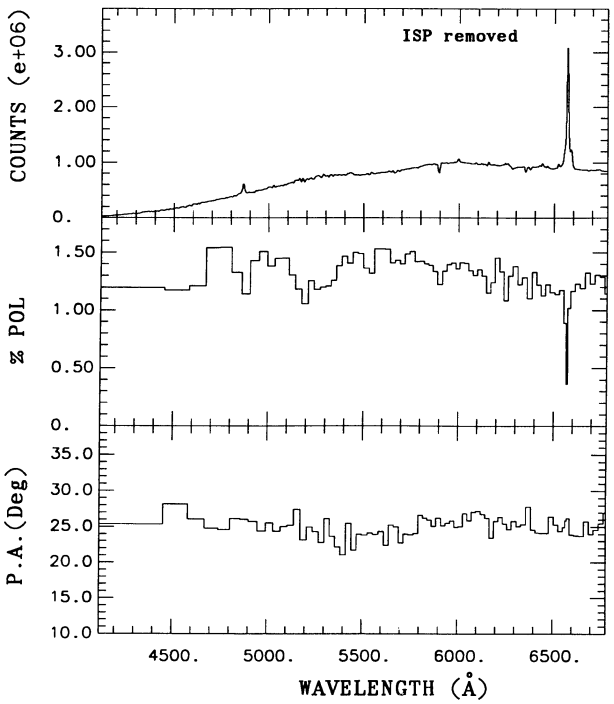

FIG. 7.—Intrinsic polarization of the AAT data

In Figure 8, we plotted the unbinned spectrum of the polarized flux of R127, which is just the polarization times the flux. Overplotted (at a different scale) is the flux spectrum. The polarized-flux spectrum can be interpreted as the spectrum of the continuum as seen by the scatterer. If the scatterers are electrons, we expect the slope of the polarized flux spectrum to agree with the continuum slope of the flux spectrum, which appears to be the case. Any opacity that competes with the electron scattering opacity on the path of the light is expected to result in spectral features in the polarized flux spectrum which may or may not be present in the flux spectrum. Figure 8 shows that the polarized flux across Hα remains constant on average, i.e., neglecting the apparent variations of polarized flux in individual pixels within the resolution of the spectrum. This was expected because the Hα polarization was used to derive the ISP correction. The polarized flux across the Fe II region can be regarded as featureless or a marginal depression; within the uncertainties outlined above we cannot assess the presence of a feature. There is a weak polarized-flux absorption feature at Hβ. This could be explained with underlying "pseudophotospheric" absorption, which is seen by the scatterers, but swamped in the flux spectrum by the emission from farther out in the wind and nebula. Finally, the most prominent feature that occurs in the polarized-flux spectrum is a strong absorption coinciding with the Na I D lines blend.

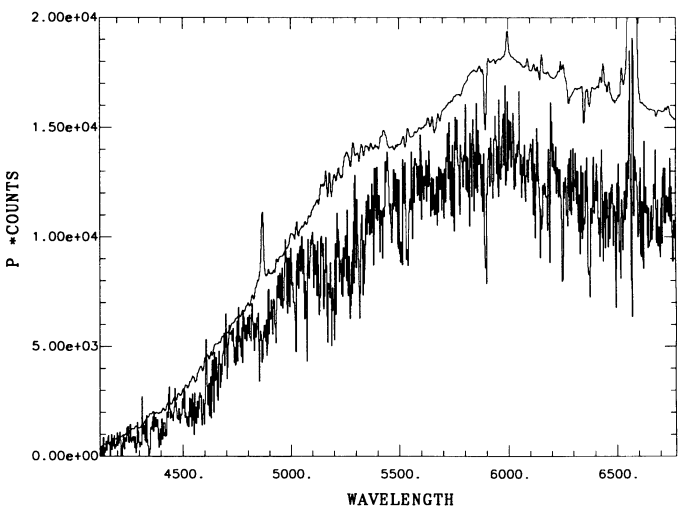

FIG. 8.—The noisy spectrum is the spectrum of the polarized flux, $P \times$ counts vs. wavelength in Å, of R127. Overplotted (on a different scale) is the counts spectrum. The spectral slopes in the continuum are the same, indicating that the scattering is due to electrons. The most prominent feature in the polarized flux spectrum is associated with Na I D. There is no feature at Hα in the polarized counts; we assumed that this line is unpolarized. There is a weak absorption feature in the polarized counts at Hβ, which is expected because of "pseudo-photospheric" absorption seen by the scatterers; in the counts spectrum, it is swamped by the circumstellar emission.

4. DISCUSSION

According to the light curve of Wolf (1992) and the visual photometry published thereafter by the Royal Astronomical Society of New Zealand (RASNZ) for 1991 August through October (Bateson 1991), R127 was still at, or in the early decline from, its 1986 maximum at the times of our observations. He I lines had been noted to disappear between 1984 August and 1986 August (Wolf et al. 1988), at the onset of the new maximum phase. Our spectrum is very similar to the 1991 January 27 spectrum published by Wolf (1992). The absence of He II and probably also He I lines in our spectrum indicates in fact that R127 was still near maximum. This suggests that the temperature of the equivalent A photosphere remained basically unchanged until late 1991. The Balmer lines originate from the wind and there will have also been a contribution of emission from the extended H II region surrounding R127 in the observing apertures. The very rich metal-line spectrum of transitions with a variety of low excitation potentials indicates that these lines form over a range of stellar radii. The forbidden lines of [N II] and [S II] are considered to form throughout the outer wind and in the H II region, because they require low densities. The densities are consistent with a recombination time scale of the order of 100 yr in the shell of R127.

The continuum polarization is expected to originate from electrons located very close to the star, within about 2 stellar radii (e.g., Rudy 1978; Cassinelli, Norksieck, & Murison 1987). In P Cyg, the largest observed intrinsic polarization, i.e., after subtraction of ISP, was 0.48% (Taylor et al. 1991); its variability on time scales down to a day is considered proof that the polarizing region(s) are indeed located near the star. The amount of intrinsic continuum polarization observed in R127, up to 1.5%, indicates both the presence of a substantial quantity of free electrons even in the wind of this equivalent A star and a very large deviation in their distribution near the star from spherical symmetry. Compared with P Cyg, this is an enormous polarization. Such high polarizations are reminiscent of what is observed in Be stars ($P \leq 2\%$), where they can be produced easily in globally axisymmetric envelopes such as equatorial disks or polar plumes and also in very oblate, geometrically thin ellipsoidal envelopes with an optical depth of around 1 (Fox 1991).

In Figure 4, we indicated the location of the tip of the maximum ISP vector, which defines a reference zero point for the Q-U parameters of the intrinsic polarization. We drew lines from this new origin through the (mean) locations of the data.

It can be seen that the amount of intrinsic continuum polarization illustrated by the distance from this new zero point to the mean locations of the three sets of observations is variable as a function of time. The intrinsic V filter polarization of our broad-band data yields $P = 1.02\%$, $\sigma \geq 0.05\%$ (the measurement error is a lower limit owing to the unknown error in the ISP correction), PA = 37°.1; simulating this filter in the spectropolarimetry gives measures of $P = 1.37\%$, $\sigma \geq 0.009\%$, PA = 24°.4. The amount of instrinsic $\%P$ variations seen in R127, 0.35%, is comparable to that seen in P Cyg, 0.44%. The variations in the amount of polarization indicate that the physical state of the stellar-wind material or its geometry or both are time-dependent. The PA of the intrinsic polarization is variable also, suggesting that the variations are at least in part due to a change of the geometry of the system.

The variations could be due to binarity. Brown, McLean, & Emslie (1978) showed that the polarization from a binary revolving in a nonspherical, Thomson-scattering envelope generally traces a Lissajous figure as a function of orbital period in Q-U space. We could interpret our data as part of such a figure. If our data are consecutive points on such a track, the orbital period exceeds 1 yr. A binary scenario is attractive because about half of all stars observed are members of binary systems and because theories already exist for the axisymmetric shells observed around novae which could perhaps be modified to explain the shells created by LBV eruptions (e.g., Gallagher 1992). A much larger body of data will be needed to test the binary hypothesis.

Alternatively, the polarization variations can be interpreted to imply changes of the free-electron density distribution in the stellar wind of a single star. These could be due to true density perturbations, or temperature fluctuations. Such changes might result in variations in the fraction of wind material that is ionized near the star. (This might cause $\%P$-spectrum changes in the optical which could be investigated with more data.) We established that the temperature of the pseudo-photosphere of R127 remained basically unchanged during the outburst, and are thus led to consider changes in wind density as the likely cause for the polarization variations. The hypothesis that the polarimetric variations are caused by changes in the mass-flow properties is consistent with the variations in velocity and strength of the P Cygni profiles observed in the maximum spectra by Wolf et al. (1988), which are generally interpreted as discrete shell ejections. While P Cygni absorption troughs measure only material seen in projection onto the stellar disk and are thus insensitive to the global wind geometry, the polarization data place additional geometric constraints on these events, by ruling out spherically symmetric shell in favor of incomplete shell or blob ejections.

In P Cyg, the intrinsic PA of the polarization is highly variable and sweeps through all four quadrants of the Q-U diagram. It is thought that the wind geometry of P Cyg is globally nearly spherical or only slightly flattened, i.e., integrated over a long time the distribution of all density fluctuations would be almost spherical or marginally flattened (see Fig. 10 of Taylor et al.). We note that the three polarimetric data sets of R127 are all confined to within one quadrant of the Q-U diagram. While this might be a chance artifact of limited temporal sampling, the PA variations of the polarization could also be interpreted to indicate a highly nonspherical, global distribution of the ensemble blobs. Mass ejections into directions limited by the opening angle of the polar plumes or the thickness of the equatorial disk about the preferred axis of the system would cause the PA of the polarization to vary within a limited range about a mean PA. The large amount of intrinsic polarization observed in R127 compared to P Cyg is again used as an important argument if favor of a large deviation from spherical symmetry of the global geometry. An ensemble of randomly distributed blobs in a globally spherical wind will cause polarization cancellation, so that the net polarization is small. This is because the polarization created by clumps in one quadrant of the stellar wind is perpendicular to that of blobs in the adjacent quadrant and their polarizations subtract vectorially. Blobs permeating a bidirectional flow will instead yield high polarizations, because the lack of clumps in adjacent quadrants will prevent cancellation. If the wind is axisymmetric, however, the presence of P Cygni profiles becomes a constraining factor of the aspect angle. Our line of sight must pass though the plane of symmetry of the wind in order for P Cygni absorptions by clumps to be seen and hence a large inclination is required.

The images of the resolved nebula of R127 (Stahl 1987; Clampin et al. 1992) show the presence of two emission enhancement along a PA of $\sim 100°$ with an opening angle each of $\sim 90°$. The mean PA of our data is $\sim 25°$ ($\pm 13°$) and this is conspicuously perpendicular to the pattern seen in the nebula, especially if we consider that we may not have quite found the "true" mean PA due to the limited sampling of Q-U space with our data. This possible 90° offset indicates that the plane of the scattering material near the star which causes the polarization may be at the same PA as the axis joining the bright emission regions of the old shell. The nebular emission patches are so symmetrical that any bi-"polar" nebula would have to be oriented at a high inclination and at an azimuth that puts the front and back lobes into the plane of the sky. Alternatively, the geometry could be that of a disk or ring of material seen nearly edge-on. If the stellar wind shares these geometric properties, we can explain the presence of high polarization and still account for the occurrence of P Cygni profiles. It is possible that the nebular features are aligned along the polar axis of the star and that the polarization originates from scattering in bipolar plumes of gas. This could make it easier to explain the large amount of free electrons detected around a relatively cool star, because the local temperature of the polar regions will be higher than that of the equatorial regions in a rapidly rotating star. The bright nebular patches are then intrepreted as regions which have been seeing a hotter radiation field. On the other hand, if the polarization originates in an equatorial disk around the star, then the nebular features too are located in the equatorial plane of the star. This would require the bright nebular patches to be density enhancements. Areas of high surface brightness in emission nebulae are usually explained with high-density regions. We consider an equatorial disk to provide the simplest picture of the geometry of the inner stellar wind and the extended nebula. A cartoon of the circumstellar environment of R127 is given in Figure 9.

A disk like structure around R127 may also provide an explanation for the *inverse* P Cygni profiles recently observed by Wolf (1992). Extensive monitoring of numerous singly ionized metal lines in the spectra of S Dor (Wolf & Stahl 1990) and R127 (Wolf 1992) revealed the presence of both variable blue and redshifted absorptions. Wolf (1992) proposed a model in which the redshifted absorptions are formed in an infalling inner envelope. In this scenario, an LBV undergoes occasional quasi pulsations, with matter escaping from the gravitational field or falling back to the photosphere.

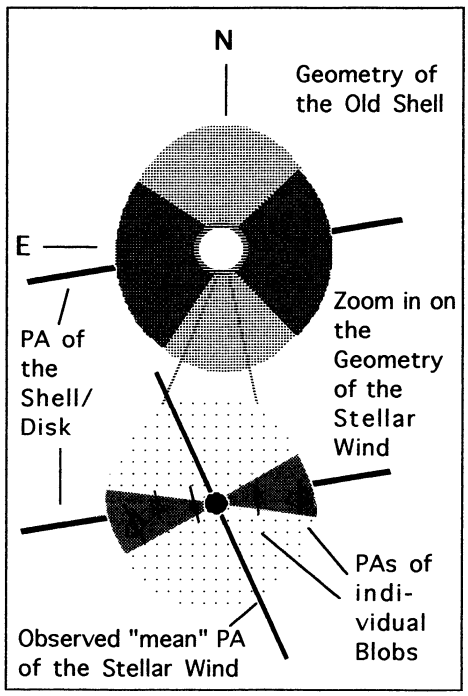

FIG. 9.—Cartoon of our picture of the geometry of the resolved shell and that of the stellar wind of R127.

Alternatively, the observed line profiles can also be interpreted in terms of a circumstellar disk. We note that the morphology of these profiles is quite reminiscent of the case of Be stars (cf. Doazan 1982). The well-monitored LBV S Dor, for instance, showed strong classical P Cygni profiles in numerous singly ionized lines of iron-group elements in 1987 November (see Wolf 1992). By 1989 January, some lines developed weak redshifted absorption components, which became comparable in strength, or even stronger, than the blue absorption components of the P Cygni profiles by 1989 December. Around 1990 September, the red absorptions mostly dominated the profiles, generating the impression of an inverse P Cygni profile. Four months later, the red absorption components had nearly disappeared. Such behavior is very similar to what is observed in classical Be stars undergoing shell ejections. In fact, the line profile of Fe II (27) λ4233 of S Dor on 1990 September 11 closely resembles the Hγ profile of the Be star 59 Cyg on 1974 September 22 (Barker 1982). The line profiles of 59 Cyg, as well as those of S Dor and R127, can be interpreted in terms of an underlying absorption with a superposed narrow shell emission mimicking an "inverse" P Cygni profile. The profiles differ with respect to the width of the underlying absorption. This, however, may be a consequence of the smaller stellar radius, and therefore higher rotational velocity of the disk, of 59 Cyg.

In our proposed model of R127—and S Dor—, redshifted absorptions do not indicate infall of matter but rather rotation. Depending on the density of the stellar wind, the inner disk like structures may sometimes, or even mostly, not be visible. This may have been the case in 1987 November, when very pronounced P Cygni profiles (without red components) in S Dor resulted from excessively high wind density. Subsequently, the mass-loss rate decreased, leaving a narrow shell line as a signature of the previous mass-loss episode superposed on the disk absorption. An interpretation of the velocity shifts of the absorptions in terms of rotational velocity instead of velocity perpendicular to the stellar surface avoids the time scale problem inherent in an "infall" model for S Dor or R127. The flow time scale associated with the infall phase is too long to be consistent with the hypothesis that material is still close enough to the star to enable deceleration of the outflow.

If a circumstellar disk is present in R127, the class of LBVs may be more closely related to B[e] stars than previously thought. B[e] stars are a class of luminous emission-line stars which are roughly in the same part of the H-R diagram as LBVs (Zickgraf et al. 1985). Their key property is a dense disk surrounding the central star. The evolutionary significance of B[e] stars is still poorly understood, and so far only weak links with LBVs could be established. Our results may indicate such a relation between LBVs and B[e] stars. Lamers & Pauldrach (1991) discussed the formation of outflowing disks around rapidly rotating, luminous, hot stars by bistable radiation-driven winds. They demonstrated that a bistability mechanism can explain the enhanced equatorial mass loss observed in B[e] stars. It is conceivable that this mechanism also operates in LBVs like R127. If this is correct, the disk surrounding R127 may not always be present due to the strongly time-variable physical conditions in the envelope of R127. The strong sensitivity of the optical depth of the Lyman continuum in the wind for variations of the stellar temperature (Lamers & Pauldrach 1991) may trigger or inhibit the formation of a disk.

Alternatively, disk formation is also predicted in magnetic rotator models for hot stars such as Be and Wolf-Rayet stars (e.g., Underhill & Fahey 1984; Poe, Friend, & Cassinelli 1989). LBVs, just like other stars, are born out of interstellar matter which is permeated with a magnetic field. Although LBVs are considered to be evolved, some may still be very young objects provided that their natal luminosity was high enough so that the Humphreys-Davidson limit acted as a barrier to halt their redward evolution into the region of the red supergiants. Present-day stellar cores which are rotating rapidly and which do still possess a significant magnetic field could be a natural consequence in the high-luminosity LBVs like R127. Such LBVs could perhaps maintain axisymmetric winds throughout their short lifes. In support of this hypothesis we note that the intrinsic position angle of the polarization of R127 falls within the range of position angles, 0–40°, found by Schmidt (1976) to characterize the interstellar polarization and thus the interstellar magnetic field of the LMC bar region. We also consider this to be the reason why the average polarization of field stars in the vicinity of R127 is parallel to the intrinsic polarization of R127.

Our polarimetric data show that a connection may exist between the geometry of the present-day stellar wind and that of the eruption which created the old shell. We thus argue in favor of a stellar origin for both. Specifically, the old shell does not seem to be the result of interaction of the outflow with the interstellar medium around the star. We could, however, explain the geometry of the shell if the underlying star *has always had* an axisymmetric wind. Recent models for the formation of the ring around SN 1987A (e.g., Eriguchi et al. 1992) indicate that even a mild asphericity in the stellar wind of the SN progenitor during the red supergiant phase, combined with rotation, will result in a large asphericity of the fast wind shed when the progenitor returned to the blue supergiant phase before it exploded. We note that LBVs, due to their high luminosity, always possess strong radiation-driven stellar winds.

However, during the LBV eruption the mass loss is considered to be much increased. We here propose to identify the ever-present, latitude-dependent LBV wind with the "seed" for the formation of an axisymmetric shell during the LBV eruption.

There now exist indications that outflows from luminous, blue stars of various classes are not spherically symmetric. Examples of such objects are the B[e] stars (Zickgraf 1992), some Wolf-Rayet stars (Schulte-Ladbeck, Meade, & Hillier 1992), and some LBVs. It will be interesting to see whether evolutionary connections between these objects can be made based on the temporal variability and the morphology of their stellar winds.

5. CONCLUSIONS

We obtained measurements of the linear polarization of R127 in the bright state. We demonstrated that the stellar-wind material within a few radii of the star is not distributed spherically symmetically around the star, and that it is time-dependent. The time dependence confirms observations of variable line profiles at maximum obtained by other groups (Wolf and collaborators). The asphericity of the wind is a new result; it rules out spherical-shell ejections. The variability amplitude of the $\%P$ is similar to what has been found in the LBV P Cyg by Hayes, Lupie, & Nordsieck, and Taylor et al., suggesting that the density perturbations are of a similar scale/density contrast in both objects. The total amount of intrinsic polarization of R127 is much larger than what has been deduced for P Cyg. The asymmetries should be larger, and could be explained by a global distortion of the wind, perhaps in the form of a rotating, circumstellar disk. The fact that the observed changes in the line spectrum are consistent with such a model gives some confidence in our suggestion. Images of R127 taken by Stahl and Clampin et al. show the presence of two bright nebular patches of emission in the extended, old shell surrounding R127. The axis joining these two regions is roughly perpendicular to the mean position angle of the polarization data. We suggest that there may be a connection between these geometries. This would require that the symmetry-breaking takes place close to the star, not in the interstellar medium into which the stellar wind expands. The asymmetry must have been present and stable for at least the last 4×10^4 yr (the age of the old shell). However, both additional polarization observations and more direct imaging with high spatial resolution will be needed to substantiate this proposition.

We thank the staff of the European Southern Observatory and the Anglo-Australian Observatory, particularly H. Schwarz, J. Bailey, and F. Freeman, for their assistance with the observations and data reduction. Data analysis was performed with a software package developed at the University of Wisconsin (K. H. Nordsieck and M. R. M.). R. S.-L. and G. C. C. thank R. Cannon for granting a director's night at the AAT. R. S.-L. acknowledges support from the STScI Visitor Program, which faciliated our collaboration on this paper. We thank M. Clampin for showing us coronographic images of R127 prior to publication. This work was supported by NAS2-56777 and NAGW-2238.

REFERENCES

Appenzeller, I., Wolf, B., & Stahl, O. 1987, in Instabilities in Luminous Early Type Stars, ed. H. J. G. L. M. Lamers & C. W. H. de Loore (Dordrecht: Reidel), 241
Barker, P. K. 1982, ApJS, 49, 89
Bateson, F. 1991, RAS New Zealand, Var. Star Sect. Circ.
Brown, J. C., McLean, I. S., & Emslie, A. G. 1978, A&A, 68, 415
Cassinelli, J. P., Nordsieck, K. H., & Murison, M. A. 1987, ApJ, 317, 290
Clampin, M., Golimowski, D., Nota, A., Leitherer, C., & Durrance, S. 1992, ApJ, submitted
Clayton, G. C., Martin, P. G., & Thompson, I. 1983, ApJ, 265, 194
Conti, P. S. 1984, in IAU Symp. 105, Observational Tests of Stellar Evolution Theory, ed. A. Maeder & A. Renzini (Dordrecht: Reidel), 233
Doazan, V. 1982, in B Stars with and without Emission Lines, ed. A. Underhill & V. Doazan (NASA SP-456), 279
Eriguchi, Y., Yamaoka, H., Nomoto, K., & Hashimoto, M. 1992, ApJ, 392, 243
Fox, G. K. 1991, ApJ, 379, 663
Gallagher, J. S. 1992, in Nonisotropic and Variable Outflows from Stars, ed. L. Drissen, C. Leitherer, & A. Nota (Provo: Brigham Young Univ. Press), 388
Gaviola, E. 1950, ApJ, 111, 408
Hayes, D. P. 1985, ApJ, 289, 726
Humphreys, R. M., & Davidson, K. 1979, ApJ, 232, 409
Hutsemékers, D., & Van Drom, E. 1991a, A&A, 248, 141
———. 1991b, A&A, 251, 620
Jeffrey, D. J. 1991, ApJ, 375, 264
Johnson, R. H., Barlow, M. J., Drew, J. E., & Brinks, E. 1992, MNRAS, 255, 261
Kurucz, R. L. 1979, ApJS, 40, 1
Lamers, H. J. G. L. M. 1987, in Instabilities in Luminous Early Type Stars, ed. H. J. G. L. M. Lamers & C. W. H. de Loore (Dordrecht: Reidel), 99
Lamers, H. J. G. L. M., & de Loore, C. W. H. 1987, Instabilities in Luminous Early Type Stars (Dordrecht: Reidel)
Lamers, H. J. G. L. M., & Pauldrach, A. W. A. 1991, A&A, 244, L5
Lupie, O. L., & Nordsieck, K. H. 1987, AJ, 92, 214
Mathewson, D. S., & Ford, V. L. 1970, AJ, 75, 778
McLean, I. S. 1977, A&A, 55, 347
Nota, A., Leitherer, C., Clampin, A., & Gilmozzi, R. 1991, in IAU Symp. 143, Wolf-Rayet Stars and Interrelations with Other Massive Stars in Galaxies, ed. K. A. van der Hucht & B. Hidayat (Dordrecht: Kluwer) 561
Paresce, F., & Nota, A. 1989, ApJ, 341, 83
Poe, C. H., Friend, D. B., & Cassinelli, J. P. 1989, ApJ, 337, 888
Rudy, R. J. 1978, PASP, 90, 668
Schmidt, Th. 1976, A&AS, 24, 357
Schulte-Ladbeck, R. E., Meade, M. R., & Hillier, D. J. 1992, in Nonisotropic and Variable Outflows from Stars, ed. L. Drissen, C. Leitherer, & A. Nota (Provo: Brigham Young Univ. Press), 118
Stahl, O. 1987, A&A, 182, 229
Stahl, O., & Wolf, B. 1986, A&A, 158, 371
Stahl, O., Wolf, B., Klare, G., Cassatella, A., Krautter, J., Persi, P., & Ferrari-Toniolo, M. 1983, A&A, 127, 49
Taylor, M., Nordsieck, K. H., Schulte-Ladbeck, R. E., & Bjorkman, K. S. 1991, AJ, 102, 1197
Thackeray, A. D. 1950, MNRAS, 110, 524
Underhill, A. B., & Fahey, R. P. 1984, ApJ, 280, 712
Walborn, N. R. 1977, ApJ, 215, 53
———. 1982, ApJ, 256, 452
Whittet, D. C. B., Martin, P. G., Hough, J. H., Rouse, M. F., Bailey, J. A., & Axon, D. J. 1992, ApJ, 386, 562
Wolf, B. 1992, in Nonisotropic and Variable Outflows from Stars, ed. L. Drissen, C. Leitherer, & A. Nota (Provo: Brigham Young Univ. Press), 327
Wolf, B., & Stahl, O. 1990, A&A, 235, 340
Wolf, B., Stahl, O., Smolinski J., & Cassatella, A. 1988, A&AS, 74, 239
Zickgraf, F. J. 1992, in Nonisotropic and Variable Outflows from Stars, ed. L. Drissen, C. Leitherer, & A. Nota (Provo: Brigham Young Univ. Press), 75
Zickgraf, F. J., Wolf, B., Stahl, O., Leitherer, C., & Klare, G. 1985, A&A, 143, 421